Near-Infrared Illumination Add-On for Mobile Hand-Vein Acquisition

Luca Debiasi, Christof Kauba, Bernhard Prommegger and Andreas Uhl
University of Salzburg
Jakob-Haringer-Str. 2, 5020 Salzburg, AUSTRIA
{ldebiasi, ckauba, bprommeg, uhl}@cs.sbg.ac.at

Abstract

There is a growing need for mobile authentication solutions. Biometric recognition systems provide several advantages over conventional knowledge and token based solutions. Especially the use of vascular patterns as a biometric trait gains more and more attention. We present a near-infrared illumination add-on for smartphone devices which allows to capture the vascular pattern of the hands (hand-veins). This device is connected and controlled via Bluetooth and customised for the Nexus 5 smartphone but can be easily adopted to fit other models too. Due to the inherent risk of fraudulent authentication attempts on a non-trusted platform like a smartphone, we propose a challenge-response approach to ensure the authenticity of the captured hand-vein images. A hand-vein data set comprising of 31 subjects and 920 images in total is acquired with the presented device. A performance evaluation utilising different hand-vein recognition schemes is conducted to show the applicability of our device and the proposed challenge-response approach.

1. Introduction

Mobile authentication solutions enjoy a wide-spread use nowadays. No matter if for payment transactions, unlocking a mobile device or identity verification at border control, there is a growing need for mobile authentication solutions. Especially the application of biometric recognition technologies in the scope of mobile authentication is gaining more and more attention. Biometrics provide several advantages over traditional means of authentication in terms of resistance against forgery and user's convenience. Fingerprint recognition systems have been integrated into higher class smartphones (e.g. the Samsung Galaxy S6 and onwards, the Apple iPhone and several more) for several years now and also face as well as iris recognition systems find their way to the newest generation of smartphones (e.g. in the Samsung Galaxy S8/S8+). Beside these traditional biometric traits, vascular pattern based ones have become an emerging biometric trait during the last years. Vascular pattern based recognition (commonly denoted as vein recognition) can help to overcome some of the problems existing biometric recognition systems have. Vein based systems rely on the structure of the vascular pattern formed by the blood vessels inside the human body tissue. This pattern only becomes visible in near-infrared (NIR) light. Thus, vein based biometrics provide a good resistance to spoofing and are insensitive to abrasion and skin surface conditions. They achieve a competitive recognition performance while the user http://digital-library.theiet.org/content/journals/10.1049/iet-cvi.2010.0191convenience is at the same level as for fingerprint systems as long as the scanner is designed in an open manner. Moreover, a liveness detection can be performed easily [11] and a contactless operation is possible, which is especially important for mobile authentication solutions. This makes vein pattern based systems a valuable choice in the scope of mobile authentication.

The application of biometric recognition systems in mobile scenarios rises some problems compared to the stationary use of these systems. First of all, the acquisition process is more unconstrained (more degrees of freedom for the placement of the biometric and varying environmental conditions) compared to the stationary case, causing several recognition performance issues [4, 5, 17]. Second, the authentication process is unsupervised, enabling presentation attacks [1, 10]. Furthermore, the mobile system might not be a trusted platform, especially if the authentication is performed on the user's smartphone. This opens the door for all kinds of insertion and replay attacks to the biometric system. Hence, there is the need for presentation attack detection systems as well as methods to prove the authenticity and integrity of the biometric sample that has been captured.

In this work we present a smartphone add-on to acquire hand-vein images. In contrast to other mobile vein scanner solutions in the literature, our add-on module is basically an illumination module only, lowering its production costs compared to full-fledged scanner devices. It utilises the phones integrated camera to capture the vein im-

ages and is controlled wirelessly via Bluetooth by our custom designed capturing Android app. Thus, together with a suitable smartphone, this add-on resembles a full mobile hand-vein scanner. Unlike most previously proposed mobile scanners, our device operates fully contactless without a specifically designed device to keep the hand in a predefined position.

To cope with the inherent risks of insertion attacks, the capturing process features a challenge-response protocol based on varying illumination intensities. In this way the app is able to prove that an actual image of the vein patterns has been captured and no previously captured sequence has been inserted instead. We established a mobile hand-vein data set captured with our mobile hand-vein add-on in combination with a modified Nexus 5 smartphone that will be made publicly available. It comprises 31 subjects and 920 images in total. Based on this data set a performance evaluation using several well-established hand-vein recognition schemes is conducted in order to show the decent recognition performance that can be achieved using our mobile hand-vein scanner and to prove the effectiveness of the challenge-response approach.

The rest of this work is organised as follows: Section 2 gives an overview of related work on mobile finger- and hand-vein scanners. The details of our proposed mobile hand-vein scanner add-on, including the challenge-response protocol, and the differences to previous mobile vein scanners are described in Section 3. Section 4 presents the publicly available data set that has been captured with our hand-vein scanner add-on. Section 5 deals with the performance evaluation. At first the details of the employed hand-vein recognition tool-chain are described, followed by the evaluation results and a results discussion. Section 6 concludes this paper and gives an outlook on future work.

2. Related Work

This section gives an overview on related work in mobile and embedded finger- as well as hand-vein scanner devices. Liu et al. [13] proposed a "a real-time embedded finger-vein recognition system for authentication on mobile devices". Their scanner consists of an NIR sensitive monochrome camera with an additional NIR pass-through filter, a white acrylic plate where the finger is placed onto and a NIR laser based illuminatior below this plate (light transmission principle). They equipped the NIR lasers to cope with problems due to shadows caused by the LED light source within their scanner design. Their full-fledged recognition system is implemented on a DSP (digital signal processor) and features image acquisition, ROI (region of interest) extraction, feature extraction and comparison. The DSP integration enables a mobile application. Sierro et al. presented three prototype touch-less vein scanners, a finger- and two palm-vein ones in [19]. The touch-less nature makes this system more convenient for the user and less susceptible to spoofing. All their proposed scanners are based on the reflected light principle (illumination source and camera on the same side of the hand/finger). Their first palm-vein prototype contains a Sony ICX618 659x494 CCD camera together with a 920 nm long-pass filter, 20 940 nm NIR LEDs and an ultrasonic sensor to detect the distance between the scanner and the hand. Their second palm-vein prototype features multi-spectral acquisition to increase its robustness against simple types of spoofing attacks by equipping blue and far-red LEDs in addition to the NIR ones. The layout of the LED positioning was changed too, but all other components are the same as within their first prototype. The finger-vein prototype consists of a OV7670 Color 640x480 pixel CMOS sensor in combination with a wide angle 2.1 mm lens and an infrared long-pass filter with a low cut-off wavelength of 740 nm. The 12 NIR LEDs are arranged in three groups of 4 LEDs each to enable an optimal illumination of the finger-veins. All three proposed scanners are small in size. The finger-vein one is USB-host powered and can be controlled by an Android app which facilitates its use as mobile finger-vein scanner. The palm-vein ones can be modified to be USB-host powered and work in combination with a smartphone too.

Eng and Khalil-Hani proposed several versions of a FPGA-based vein biometric authentication system. In [3] they introduced an embedded hand vein scanner implemented on an Altera Nios II prototyping system running on Nios2-Linux as real time operating system. Their sensor consists of an reflected light source (NIR LED array), a modified thermal webcam with a resolution of 320x240 pixels and an attached IR filter. They captured images from the dorsal (back) side of the hand and utilised minutiae based features extracted from the vein pattern for recognition. In [8] and [9] they proposed two versions of a finger vein recognition system. Again, the system was implemented on an Altera prototyping system running Nios2-Linux using a modified webcam. Contrary to the hand vein scanner, they used the light transmission method to acquire images from the palmar side of the finger. For recognition they use minutiae based methods again.

Lee et al. presented a mobile multimodal biometric capture device utilising finger-veins and fingerprints in [12]. Their scanner consists of two QuickCam USB cameras, a visible light source for fingerprints and four 880 nm NIR LEDs for finger-veins using the light transmission principle. The captured images have a resolution of 640x480 pixels. Their embedded system unit is a ultra mobile processing computer manufactured by SONY Corp (VGN-UX17LP). They used a minutiae based recognition method for both, finger-veins and fingerprints.

Fletcher et al. proposed two mobile hand-vein scanners in [4]. The first one uses an unmodified Sony Experia

Mini Pro Android smartphone as camera. The light source consists of 16 NIR LEDs with an operation frequency of 850 nm. They used a Kodak Wratten filter (#87) with a pass-through frequency range of 740-795 nm as optical filter. The second one uses a Gearhead Nightvision webcam (WC1100BLU) which already contains six IR LEDs as light source. For a better illumination they replaced the internal LEDs with 940 nm NIR LEDs. Again, they used a Kodak Wratten filter (#87c) with a pass-through frequency range of 790-855 nm as optical filter. The webcam is attached to a Nexus 7 Android tablet. Both scanners used especially designed apparatuses to place the hand into a well defined position. They acquired the vein structure from the palmar side and used minutiae based features for biometric recognition.

In contrast to existing mobile hand- and finger-vein scanners, our proposed mobile hand-vein scanner is basically an illumination add-on module for smartphones. Thus, it exhibits lower production costs compared to a full featured scanner device.

3. Mobile Hand-Vein Scanner Add-On

As mentioned in Section 2, the basic components of a hand-vein scanner are an NIR light source and an NIR-sensitive image sensor (camera). Every common smartphone nowadays has a built-in camera, which is sufficient to capture high-resolution hand-vein images. However, these cameras are usually equipped with NIR blocking filters in order to avoid unwanted colour effects in the captured images. Thus, it is necessary to either remove this NIR blocking filter, like it has been done for the modified Nexus 5 smartphone by EigenImaging (`https://www.eigenimaging.com/`) we utilised, or a separate NIR-sensitive camera has to be equipped in the smartphone. The latter is done by some manufacturers already (e.g. Samsung for iris recognition) and it is likely that others will follow this trend. If the smartphone already contains an NIR-sensitive camera, it can be utilised for hand-vein recognition and the only additional component needed is the NIR light source.

Our mobile hand-vein scanner add-on is essentially such a light source in the form of an add-on module for smartphone devices, depicted in Fig. 1. It is the first mobile hand-vein scanner device of its kind, exhibiting lower production costs compared to previous mobile finger- and hand-vein scanners as it does neither contain a separate image sensor nor a complex control board. The whole device was designed to be used in combination with our modified Nexus 5 smartphone utilising its integrated camera as image sensor and has been constructed by ourselves. The housing part, where the smartphone is slid in, consists of several, 3D printed components. Hence, it can be easily modified for other smartphone models. This control board is based on

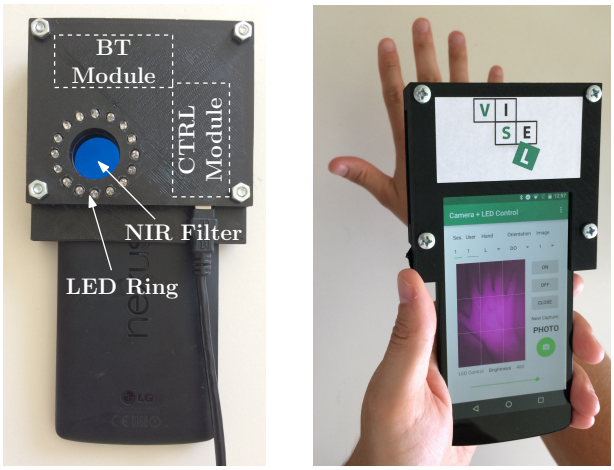

Figure 1: Left: mobile hand-vein scanner add-on, right: typical acquisition set-up

an Arduino Nano Board (`https://store.arduino.cc/arduino-nano`), a Bluetooth module and a 16 channel LED driver IC. The control board design was adopted from our previous finger-vein scanner [6] and modified for the mobile application. It does not require a physical cable connection to the smartphone, the data transfer and control is achieved via Bluetooth communication. The USB cable on the prototype is only needed for power supply, but the final version will have a built-in rechargeable battery. It has 16 NIR LEDs with a peak wavelength of 850 nm that are arranged in a circle around the smartphone's camera. Each LED can be brightness controlled individually. This enables a uniform and sufficient illumination for the hand-vein images on the one hand and provides the ability to use complex illumination patterns for encoding information on the other hand. Moreover, our add-on is equipped with an NIR pass-through filter having a cut-off frequency of 780 nm to filter out the ambient light and to improve the image contrast.

The LED brightness is automatically controlled by a capturing app running on the smartphone, prior to the acquisition of a single image. Currently, the app only supports the capturing of single images as well as video sequences of the hand-veins, no feature extraction and comparison is done yet. This is why it is currently an add-on for the acquisition of hand-vein images and not for performing a full authentication.

3.1. Challenge-Response Protocol

In order to prevent presentation and replay attacks, the developed mobile hand-vein scanner add-on is capable of performing challenge response (CR) authentication due to its 16 fully controllable NIR LEDs.

Presentation attacks for finger veins have already been successfully conducted in [21] by Tome et al., where

a spoofing false accept rate of 85% has been achieved. Their experiments have been conducted using an extensible framework for spoofing finger veins, which might also be successfully applied to hand veins.

CR authentication follows the simple principle that one party presents a question, i.e. the *challenge*, to which another party has to provide a valid answer, i.e. the *response*, in order to pass the authentication. In [20] Stein *et al.* proposed a video-based fingerprint recognition and anti-spoofing solution for smartphones. They developed a CR protocol, where the finger needs to be moved towards the camera and the reflectance of the finger surface is measured.

In the scenario presented here, the first party (user) tries to authenticate itself in a biometric system using his/her smartphone. More precisely, the smartphone is used as a mobile sensor to acquire the user's biometric trait, i.e. the vascular pattern of the hand, and the data is then submitted to the biometric system wirelessly for the identification. Since the smartphone cannot be trusted, as mentioned in Section 1, the biometric system has to ensure the authenticity and up-to-dateness of the acquired biometric data to prevent a malicious insertion or spoofing of the submitted data, i.e. presentation and replay attacks. Therefore, a video of the hand is acquired for authentication, which contains a blinking sequence generated based on a specific challenge using the 16 fully controllable NIR LEDs. This blinking sequence is an inherent part of the video, which is sent to the biometric system after acquisition. This ensures that the response is interwoven with the biometric data.

The proposed challenge response protocol consists of the following steps:

1. The smartphone sends an authentication request to the biometric system.
2. The biometric system generates a random number which defines a fixed blinking sequence and sends it to the smartphone (challenge).
3. The smartphones generates a blinking sequence based on the random number and controls the 16 LEDs accordingly. In parallel, a video of the hand (dorsal or palmar) is recorded.
4. The video containing the biometric data and blinking sequence (response) is sent wirelessly to the biometric system.
5. The biometric system detects the blinking sequence and compares it to the previously generated random number.
6. If the response matches the challenge, the hand vein recognition is performed and the user is authenticated. Otherwise, the whole process is repeated.

We implemented this challenge response protocol in form of an Android application, which runs on the user's smartphone. The app consists of two major parts: The video recording and the LED control. The video recording part has been realised using *CameraView* (`https://github.com/natario1/CameraView`), a high-level library providing access to the smartphone's camera in order to capture photos and videos. The LED control is performed via Bluetooth. The application is able to capture both photos and videos and contains different settings to configure the acquisition parameters for testing and development. The GUI of the developed application is depicted in Figure 2a.

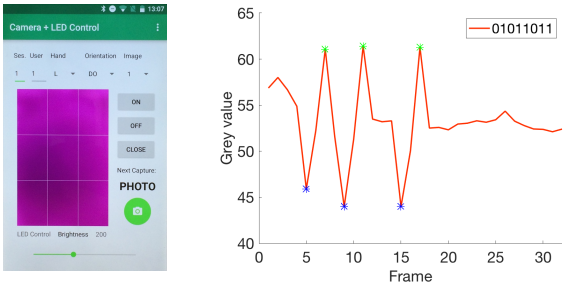

(a) GUI

(b) Grey values

Figure 2: Graphical user interface (a) of the developed Android application for LED control and capturing of photos and videos. Sequence of mean grey values (b) for an exemplary video with detected 0s (marked as blue stars around a gray value of 45) and 1s (marked as green stars around a gray value of 60).

In our first proof of concept, we generate a random number between 1 and 255, which is logged to a file for later evaluation. This random number, which by concept would be sent by the biometric system, is then transformed into an 8-bit binary sequence: For 0 the brightness of the LEDs is reduced to half of its intensity, while for 1 the intensity is kept at a predefined level. All LEDs are controlled equally in the current version, but multiple illumination zones can be realised in the future to enable more complex blinking sequences. For this work, we acquired videos with a duration of 3 seconds containing the 8-bit sequence, leading to a blinking interval duration of 375 ms. For synchronisation purposes, we added a padding with a duration of 1.5 seconds before and after the blinking sequence of the video.

The biometric system, which receives the video, has only been simulated so far. Therefore, the blinking sequence is first extracted from the recorded video and compared to the previously logged random number for the specific video. For the detection of the sequence, single frames are extracted from the video at a frame-rate of 5.33 fps using FFmpeg (`https://www.ffmpeg.org`). The frame-rate has been selected in correspondence to the blinking interval of 375 ms, leading to two frames being extracted for each

blinking interval and a total of 32 frames for the whole video: 8 images of padding before and after the blinking sequence and 16 images for the sequence itself. Thereafter, the mean grey value of each extracted image is determined. Since the used camera library does not allow a manual exposure, it is automatically regulated after each blinking to obtain a certain mean grey value. Hence, we are only able to detect changes in illumination. Afterwards, the local minima and maxima, i.e. 0s and 1s, of the blinking sequence are determined from the mean grey value curve, as shown in Figure 2b. The intervals between these extrema, i.e. where no illumination change has happened, are interpolated by the preceding value. With this procedure, we obtain an 8-bit binary sequence again which is matched against the 8-bit binary sequence of the random number.

4. Mobile Hand-Vein Data Set

The mobile hand-vein data set was acquired using our mobile hand-vein scanner add-on in combination with the modified Nexus 5 smartphone. It includes dorsal as well as palmar hand-vein images of 31 individual subjects. No supporting apparatuses to place the hand in a predefined positional were used. As a result, the captured images resemble a realistic real-live scenario with all possible types of distortions like rotation, tilting in all possible directions and scaling (different distances of the hand and the smartphone). The data acquisition was split into two separated sessions, the first one outdoor inside a car and the second one indoors. Throughout the first session 28 subjects have been acquired, during the indoor session 18. 15 subjects participated in both sessions. Five images per hand and per view have been acquired, summing up to a total of 920 images. The acquisition outside was done to simulate a realistic application scenario of our mobile hand-vein add-on in a border control environment, the inside session was conducted to have reference images in a more controlled environment. The acquired colour JPEG images have a resolution of 2448x3264 pixels. We extracted square ROI patches of the hand-vein images manually, which have a resolution of 512x512 pixels. Figure 3 shows some example images. This data set will be publicly available as part of the PROTECT Multimodal DB Dataset [22] database and can be downloaded at `http://projectprotect.eu/`.

Figure 3: Example images of the mobile hand-vein data set, left: dorsal, right: palmar

5. Experimental Evaluation

In the following the finger-vein processing tool-chain and the evaluation protocol are described. Then the experimental results are given and discussed.

5.1. Processing Tool-Chain

The finger-vein processing tool-chain consists of ROI extraction, preprocessing, feature extraction and comparison. We opted for simple binarisation type feature extraction methods as well as two key-point based methods (one SIFT based and an adopted version of an algorithm proposed by Matsuda et al. in [15]) to have a complimentary feature type too.

ROI Extraction The ROI extraction is done manually by fitting a rectangular ROI is fit inside the hand area. The ROI images have a size of 512×512 pixels.

Preprocessing To improve the image contrast and the visibility of the vein pattern **CLAHE** [25], which is the most prevalent and simple technique, in combination with **High Frequency Emphasis Filtering (HFE)** [24] and filtering with a **Circular Gabor Filter** (**CGF**) as proposed by Zhang and Yang [23] are applied. Furthermore, the images are resized to half of its original size, which not only speeds up the comparison process but further improves the results due to intrinsic denoising. For more details on the preprocessing methods the interested reader is referred to the authors' original publications.

Feature Extraction and Comparison The first three of the following techniques aim to extract the vein pattern from the background resulting in a binary template image followed by a comparison of these binary templates using a correlation measure.

Maximum Curvature (MC [16]) aims to emphasise only the centre lines of the veins, making it insensitive to varying vein widths. The first step is the extraction of the centre positions of the veins. Afterwards a score according to the width and curvature of the vein region is assigned to each centre position and recorded in a matrix called locus space. Due to noise or other distortions some pixels may not have been classified correctly at the first step, thus the

centre positions of the veins are connected using a filtering operation. Finally binarisation is done by thresholding using the median of the locus space.

Principal Curvature (PC [2]): At first the gradient field of the image is calculated. Hard thresholding is done to filter out small noise components and then the gradient at each pixel is normalised to 1 to get a normalised gradient field. This is smoothed by applying a Gaussian filter. The next step is the actual principal curvature calculation, obtained from the Eigenvalues of the Hessian matrix at each pixel. Only the bigger Eigenvalue, corresponding to the maximum curvature, is used. The last step is a binarisation of the principal curvature values to get the binary vein output image.

Gabor Filter (GF [11]): The image is filtered using a filter bank consisting of several 2D even symmetric Gabor filters with different orientations, resulting in several feature images. The final vein feature image is obtained by fusing all these single images, which is then post-processed using morphological operations to remove noise.

For comparing the binary feature images we adopted the approach of Miura et al. [16]. As the input images are neither registered to each other nor aligned vertically, the correlation between the input image and x- and y-direction shifted versions of the reference image is calculated. The maximum of these correlation values is normalised and then used as final comparison score.

In addition to the techniques described above, the fourth technique is a key-point based one. Key-point based techniques try to use information from the most discriminative points as well as considering the neighbourhood and context information of these points by extracting key-points and assigning a descriptor to each key-point. We used a **SIFT** [14] based technique with additional key-point filtering along the finger boundaries as proposed by Kauba et al. [7] and a modified version of **Deformation-Tolerant Feature-Point Matching** (DTFPM) proposed by Matsuda et al. [15]. DTFPM was designed for finger-vein recognition. Its feature extraction assumes a circular shape of the finger. This does not apply for hand-vein recognition, thus we modified the feature extraction step.

5.2. Evaluation Protocol

The experiments are split into two main parts: in the first part we analyse the recognition performance of the database. For evaluation purposes, dorsal and palmar images are regarded as two independent data sets. In addition to the analysis of the two acquired sessions, we performed a comparison of session 1 against session 2 as well. To quantify the performance, the EER as well as the FMR100 (the lowest $FNMR$ for $FMR <= 1\%$), the FMR1000 (the lowest $FNMR$ for $FMR <= 0.1\%$) and the ZeroFMR (the lowest $FNMR$ for $FMR = 0\%$) are used. We applied the following test protocol: For calculating the genuine scores, all possible genuine comparisons are performed. For calculating the impostor scores, only the first image of a finger is compared against the first image of all other fingers. Table 1 states the number of comparisons for each evaluation. As our recognition scheme does not require a training step, no separate training and test set is needed. All result values are given in percentage terms, e.g. 1.43 means 1.43%. In the second part of our experiments, we evaluated the captured videos with respect to the challenge-response protocol described in Section 3.1. A public implementation of the complete processing tool-chain as well as the scores and detailed results are available at: `http://www.wavelab.at/sources/Debiasi18b`.

	Session 1	**Session 2**	**Session 1 vs 2**
Genuine	560	360	750
Impostor	1540	630	855
Total	2100	990	1650

Table 1: Number of matches per data set/session evaluation

5.3. Recognition Performance Results

The performance evaluation has been conducted for both, the palmar and dorsal sub-set. Figure 4 shows some sample images including te extracted MC features. In the dorsal ROI image, the vein structure is visible. In the images acquired from the palmar side (bottom row), the vein structure is not visible as prominently. The ROI image on the left side is dominated by the texture of the palm. This fact is also reflected in the extracted MC features (right side): most of the extracted lines do not result from the vein structure but from the creases and wrinkles of the skin.

Table 2 lists the results for the dorsal subset. For session 1 (outdoor) MC achieves the best result with an EER of 4.13% followed by DTFPM (7.33%), SIFT (10.63%) and PC (10.71%). With an EER of 28.08%, GF perform significantly worse than all other feature types. For session 2 (indoor, controlled ambient light) all feature types except PC perform worse. MC still shows the best performance with and EER of 5.69%. PC (8.97%) now achieves a better result than DTFPM (12.00%) and SIFT (14.17%). Again, the recognition performance of GF (36.37%) is not competitive to the other methods. For the inter-session comparison, the performance drops dramatically. MC achieves an EER of only 24.30% which is six times worse than the result for session 1. PC and DTFPM exhibit EERs around 30%, SIFT and GF of greater than 40%. The DET plots for session 1 and 2 are depicted in Figure 5 left and right, respectively.

Table 3 states the results for the palmar sub-set. The results follow the same trend as for the dorsal sub-set: MC performs best for all 3 experiments followed by DTFPM, SIFT and PC. The outdoor session exhibits a better performance than the indoor session and the inter-session comparison performs significantly worse than the single sessions.

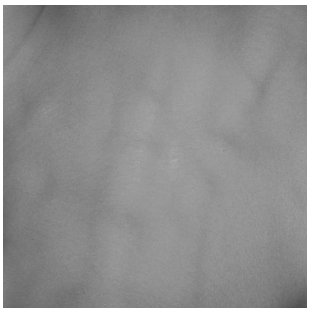

(a) ROI dorsal

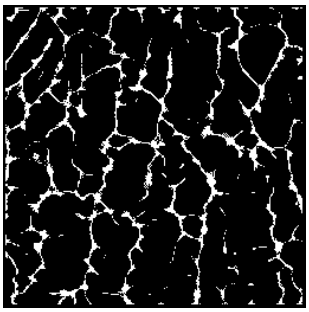

(b) Features (MC) dorsal

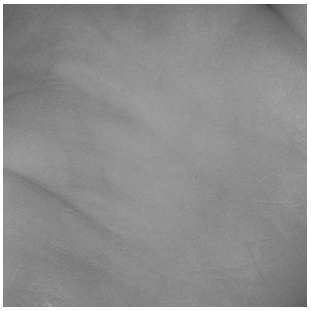

(c) ROI palmar

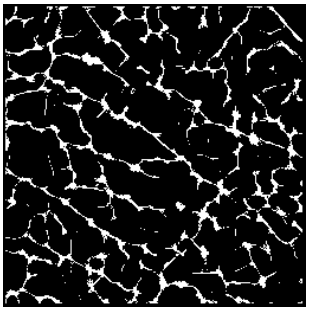

(d) Features (MC) palmar

Figure 4: Sample images of both data sets: dorsal images on the top, palmar at the bottom. The left column shows the extracted ROI, the right column the extracted MC features

Session 1				
	EER	FMR100	FMR1000	ZeroFMR
MC	**4.13 (±1.11)**	6.79	10.54	12.50
PC	10.71 (±1.72)	15.54	18.39	18.75
GF	28.08 (±2.50)	68.39	74.64	75.89
SIFT	10.63 (±1.72)	17.50	27.68	28.57
DTFPM	7.33 (±1.45)	13.04	16.61	17.32
Session 2				
	EER	FMR100	FMR1000	ZeroFMR
MC	**5.69 (±1.77)**	9.44	23.06	23.06
PC	8.97 (±2.17)	13.61	16.94	16.94
GF	36.37 (±3.66)	81.39	85.83	85.83
SIFT	14.17 (±2.65)	31.11	37.22	37.22
DTFPM	12.00 (±2.47)	23.33	28.33	28.33
Session 1 vs Session 2				
	EER	FMR100	FMR1000	ZeroFMR
MC	**24.30 (±2.49)**	56.13	69.87	69.87
PC	28.48 (±2.62)	54.13	68.00	68.00
GF	42.24 (±2.87)	96.67	99.20	99.20
SIFT	41.12 (±2.86)	88.80	94.40	94.40
DTFPM	30.22 (±2.67)	65.87	74.53	74.53

Table 2: Recognition performance results in terms of EER/FMR100/FMR1000/ZeroFMR for the dorsal sub-set for the single sessions and cross session

GF cannot compete with the other methods. The DET plots for session 1 and 2 are depicted in Figure 6.

Considering that the images have been acquired fully contactless in an nearly unconstrained environment, the recognition rate of the system for the single individual ses-

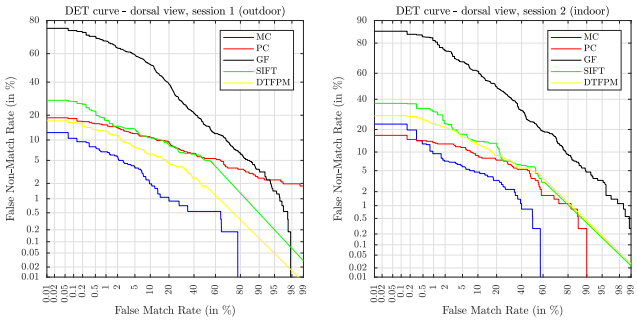

Figure 5: DET plot for session 1 (left) and session 2 (right) of the dorsal view

Session 1				
	EER	FMR100	FMR1000	ZeroFMR
MC	**7.52 (±1.47)**	10.54	13.04	13.39
PC	13.88 (±1.93)	23.75	31.07	34.64
GF	32.52 (±2.61)	85.71	90.71	93.93
SIFT	11.90 (±1.80)	21.43	34.11	39.82
DTFPM	7.67 (±1.48)	12.14	16.79	21.96
Session 2				
	EER	FMR100	FMR1000	ZeroFMR
MC	**7.78 (±2.04)**	15.28	22.78	22.78
PC	14.52 (±2.68)	21.94	24.17	24.17
GF	33.93 (±3.60)	82.22	89.17	89.17
SIFT	14.21 (±2.66)	30.28	43.61	43.61
DTFPM	12.14 (±2.49)	22.50	26.67	26.67
Session 1 vs Session 2				
	EER	FMR100	FMR1000	ZeroFMR
MC	**27.73 (±2.60)**	56.00	65.47	65.47
PC	34.27 (±2.76)	62.80	75.33	75.33
GF	42.24 (±2.87)	98.53	99.87	99.87
SIFT	41.38 (±2.86)	86.00	95.87	95.87
DTFPM	34.07 (±2.76)	76.67	85.07	85.07

Table 3: Recognition performance results in terms of EER/FMR100/FMR1000/ZeroFMR for the palmar sub-set for the single sessions and cross session

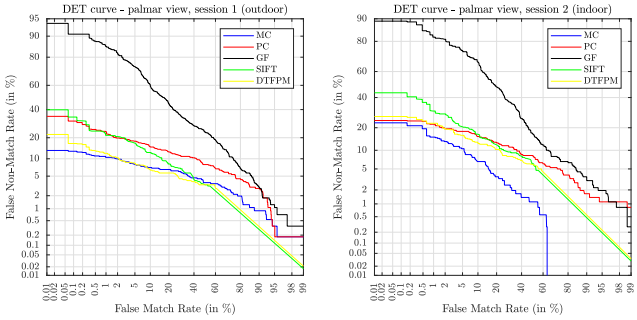

Figure 6: DET plot for session 1 (left) and session 2 (right) of the palmar view

sions is acceptably good. The inferior performance of session 2 (indoor with more controlled artificial ambient light) might be due to the proposed illumination add-on which does not provide enough NIR light to sufficiently highlight the "deeper" veins. The additional NIR light present in sun-

light might help to render the veins more visible in the outdoor session and therefore increase its recognition performance. The palmar images are dominated by the creases of the hand. The veins on the palmar side are deeper inside the skin as on the dorsal side. Our illumination does not penetrate deep enough into the tissue. Therefore, the vein structure is only partially visible. This explains the performance decrease of the palmar sub-set compared to the dorsal one.

The significant performance drop of the inter-session comparison might result from the unconstrained environment. Vein structure based methods rely on the correlation of the images. During comparison we shifted the images in x- and y-direction and rotated them in order to maximise the correlation and correct small displacements. This corrections might have not been enough as they do not consider non-planar rotations (tilt). Considering our previous work [18], one could expect that key-point based algorithms, especially DTFPM, are better suited for an unconstrained acquisition environment. The performance of these methods needs to be further investigated.

5.4. Challenge-Response Evaluation Results

The challenge-response evaluation has been conducted on a total of 65 videos for 13 different users with random blinking sequences. For this purpose, the expected binary sequences determined by the random number generated for each video have been compared to the detected binary sequences, which have been extracted by the procedure described in Section 3.1, by means of Hamming Distance (HD). A sequence has been defined as a match (M), only with a HD equal to 0. Otherwise, the detected sequence has been defined as a non-match (NM). Table 4 shows the matching accuracy and mean hamming distance for non-matches for each user. A mean detection accuracy of 0.82 has been achieved for all CR-videos with a mean HD of 3.04 for failed detection attempts. Compared to a related biometric recognition and CR solution proposed in [20], where a detection accuracy of 0.40 has been achieved in one CR authentication attempt (80 out of 201), we obtain a competitive result.

The failed detection is mainly caused by synchronisation problems, e.g. for users 3 and 10. This synchronisation problems arise from two different factors: a software factor in form of the used camera library and a hardware problem with the timing of the LEDs. The camera library causes some delay with the video acquisition, which causes a desynchronisation of the blinking intervals, while the current implementation of the embedded LED control can cause inconsistent timer intervals with a deviation of up to 200 ms. Furthermore, due to the missing manual exposure setting in the camera library, some longer consecutive sequences of 0s or 1s are not interpolated correctly. All of these issues will be addressed in future versions of the mobile hand-vein scanner add-on, by choosing another library to access the camera and changing the embedded LED control to an interrupt based control.

User	ACC	Mean HD NM
1	0.60	2
2	1.00	-
3	0.80	4
4	0.80	2
5	0.60	2.50
6	0.20	2.75
7	1.00	-
8	0.80	2
9	1.00	-
10	0.80	6
11	1.00	-
12	1.00	-
13	1.00	-
Mean	0.82	3.04

Table 4: Detection accuracy (ACC) and mean Hamming Distance for non-matches (Mean HD NM) for CR sequence detection. If $ACC = 1$ there are no non-matches, so no distance can be calculated, thus there is $-$ in the Mean HD MM column.

6. Conclusion and Future Work

We proposed an illumination add-on for smartphones which turns a smartphone with an NIR-sensitive camera into a mobile hand vein scanner device. Using such a scanner, we established a publicly available data set acquired in two time-span separated and environmental different (indoor, outdoor) sessions and analysed the recognition performance of the new data set utilising some well-established vein recognition schemes. We further proposed a challenge-response protocol in order to prevent replay and presentation attacks and evaluated its applicability.

In our future work we will further develop our illumination add-on to enhance the acquisition quality. We will look into a multi-sample fusion of the different video frames captured from the hand-veins in order to improve the recognition performance. Moreover, we aim to evolve DTFPM as a hand vein recognition scheme which is tolerant against non-planar rotations. In addition, we will continue to develop our challenge-response protocol, improve the Android app and LED controller. Furthermore, we plan to utilise the smartphone's built-in sensors to deal with some of the imposed challenges caused by the unrestricted positioning of the phone relative to the hand. After all of the mentioned improvements have been implemented, we will further extend our mobile hand-vein data set by acquiring additional subjects.

Acknowledgements

This project has received funding from the European Union's Horizon 2020 research and innovation program under grant agreement No. 700259.

References

[1] Z. Boulkenafet, J. Komulainen, Z. Akhtar, A. Benlamoudi, D. Samai, S. E. Bekhouche, A. Ouafi, F. Dornaika, A. Taleb-Ahmed, L. Qin, F. Peng, L. B. Zhang, M. Long, S. Bhilare, V. Kanhangad, A. Costa-Pazo, E. Vazquez-Fernandez, D. Perez-Cabo, J. J. Moreira-Perez, D. Gonzalez-Jimenez, A. Mohammadi, S. Bhattacharjee, S. Marcel, S. Volkova, Y. Tang, N. Abe, L. Li, X. Feng, Z. Xia, X. Jiang, S. Liu, R. Shao, P. C. Yuen, W. R. Almeida, F. Andalo, R. Padilha, G. Bertocco, W. Dias, J. Wainer, R. Torres, A. Rocha, M. A. Angeloni, G. Folego, A. Godoy, and A. Hadid. A competition on generalized software-based face presentation attack detection in mobile scenarios. In *2017 IEEE International Joint Conference on Biometrics (IJCB)*, pages 688–696, Oct 2017.

[2] J. H. Choi, W. Song, T. Kim, S.-R. Lee, and H. C. Kim. Finger vein extraction using gradient normalization and principal curvature. *Proc.SPIE*, 7251:7251 – 7251 – 9, 2009.

[3] P. C. Eng and M. Khalil-Hani. Fpga-based embedded hand vein biometric authentication system. In *TENCON 2009 - 2009 IEEE Region 10 Conference*, pages 1–5, Jan 2009.

[4] R. R. Fletcher, V. Raghavan, R. Zha, M. Haverkamp, and P. L. Hibberd. Development of mobile-based hand vein biometrics for global health patient identification. In *Global Humanitarian Technology Conference (GHTC), 2014 IEEE*, pages 541–547. IEEE, 2014.

[5] V. Kanhangad, A. Kumar, and D. Zhang. Contactless and pose invariant biometric identification using hand surface. *IEEE transactions on image processing*, 20(5):1415–1424, 2011.

[6] C. Kauba, B. Prommegger, and A. Uhl. Focussing the beam - a new laser illumination based data set providing insights to finger-vein recognition. In *Proceedings of the IEEE 9th International Conference on Biometrics: Theory, Applications, and Systems (BTAS2018)*, pages 1–9, Los Angeles, California, USA, 2018.

[7] C. Kauba, J. Reissig, and A. Uhl. Pre-processing cascades and fusion in finger vein recognition. In *Proceedings of the International Conference of the Biometrics Special Interest Group (BIOSIG'14)*, Darmstadt, Germany, Sept. 2014.

[8] M. Khalil-Hani and P. C. Eng. Fpga-based embedded system implementation of finger vein biometrics. In *2010 IEEE Symposium on Industrial Electronics and Applications (ISIEA)*, pages 700–705, Oct 2010.

[9] M. Khalil-Hani and P. C. Eng. Personal verification using finger vein biometrics in fpga-based system-on-chip. In *2011 7th International Conference on Electrical and Electronics Engineering (ELECO)*, pages II–171–II–176, Dec 2011.

[10] P. Korshunov, S. Marcel, H. Muckenhirn, A. Gonçalves, A. Mello, R. Violato, F. Simões, M. Uliani Neto, M. de Assis Angeloni, J. A. Stuchi, et al. Overview of btas 2016 speaker anti-spoofing competition. Technical report, Idiap, 2016.

[11] A. Kumar and Y. Zhou. Human identification using finger images. *Image Processing, IEEE Transactions on*, 21(4):2228–2244, 2012.

[12] H. C. Lee, K. R. Park, B. J. Kang, and S. J. Park. A new mobile multimodal biometric device integrating finger vein and fingerprint recognition. In *Ubiquitous Information Technologies & Applications, 2009. ICUT'09. Proceedings of the 4th International Conference on*, pages 1–4. IEEE, 2009.

[13] Z. Liu and S. Song. An embedded real-time finger-vein recognition system for mobile devices. *IEEE Transactions on consumer Electronics*, 58(2), 2012.

[14] D. G. Lowe. Object recognition from local scale-invariant features. In *Proceedings of the Seventh IEEE International Conference on Computer Vision (CVPR'99)*, volume 2, pages 1150 – 1157. IEEE, 1999.

[15] Y. Matsuda, N. Miura, A. Nagasaka, H. Kiyomizu, and T. Miyatake. Finger-vein authentication based on deformation-tolerant feature-point matching. *Machine Vision and Applications*, 27(2):237–250, 2016.

[16] N. Miura, A. Nagasaka, and T. Miyatake. Extraction of finger-vein patterns using maximum curvature points in image profiles. *IEICE transactions on information and systems*, 90(8):1185–1194, 2007.

[17] A. Morales, M. A. Ferrer, and A. Kumar. Towards contactless palmprint authentication. *IET computer vision*, 5(6):407–416, 2011.

[18] B. Prommegger, C. Kauba, and A. Uhl. Longitudinal finger rotation - problems and effects in finger-vein recognition. In *Proceedings of the International Conference of the Biometrics Special Interest Group (BIOSIG'18)*, Darmstadt, Germany, 2018.

[19] A. Sierro, P. Ferrez, and P. Roduit. Contact-less palm/finger vein biometrics. In *2015 International Conference of the Biometrics Special Interest Group (BIOSIG)*, pages 1–12, Sept 2015.

[20] C. Stein, V. Bouatou, and C. Busch. Video-based fingerphoto recognition with anti-spoofing techniques with smartphone cameras. In *2013 International Conference of the BIOSIG Special Interest Group (BIOSIG)*, pages 1–12, Sept 2013.

[21] P. Tome and S. Marcel. On the vulnerability of palm vein recognition to spoofing attacks. In *The 8th IAPR International Conference on Biometrics (ICB)*, May 2015.

[22] University of Reading. PROTECT Multimodal DB Dataset, June 2017. Available by request at http://projectprotect.eu/dataset/.

[23] J. Zhang and J. Yang. Finger-vein image enhancement based on combination of gray-level grouping and circular gabor filter. In *Information Engineering and Computer Science, 2009. ICIECS 2009. International Conference on*, pages 1–4. IEEE, 2009.

[24] J. Zhao, H. Tian, W. Xu, and X. Li. A new approach to hand vein image enhancement. In *Intelligent Computation Technology and Automation, 2009. ICICTA'09. Second International Conference on*, volume 1, pages 499–501. IEEE, 2009.

[25] K. Zuiderveld. Contrast limited adaptive histogram equalization. In P. S. Heckbert, editor, *Graphics Gems IV*, pages 474–485. Morgan Kaufmann, 1994.